Progress and challenges of graphene oxide/metal-organic composites

Mégane Muschi, Christian Serre

Progress and challenges of graphene oxide/metal-organic composites

Mégane Muschi[a], Christian Serre[a]

Institut des Matériaux Poreux de Paris, UMR 8004 CNRS, Ecole Normale Supérieure, Ecole Supérieure de Physique et de Chimie Industrielles de Paris, PSL University, 75005 Paris, France

Contents

Abstract

Graphene oxide (GO) coupled with inorganic materials, from 0D coordination complexes to 3D Metal-Organic Frameworks (MOFs) offer promising perspectives. The synergic effects of these two materials can lead to enhanced or even new properties. The nature of the interactions between the carbon-based material and the hybrid one strongly depends on the synthetic method. As these composites bring more and more attention, this review aims at giving a global scope of the different synthetic routes used in the literature, as well as the characterizations and applications of such systems.

Abbreviations: DNP, dynamic nuclear polarization; FTIR, Fourier transformation infra-red; GO, graphene oxide; HER, hydrogen evolution reaction; MOF, metal-organic framework; OER, oxygen evolution reaction; ORR, oxygen reduction reaction; PB, Prussian blue; PXRD, powder X-ray diffraction; rGO, reduced graphene oxide; SEM, scanning electron microscopy; TEM, transmission electron microscopy; TGA, thermogravimetric analysis; XPS, X-ray photoelectron spectroscopy.

I. Introduction

Inorganic-organic hybrid materials are widely used nowadays in commercial production, such as the sol-gel process. They also remain an active topic for fundamental research due to the efficient combination of the properties exhibited by the organic and inorganic components.[1, 2] Among them, zero-dimensional (0D) coordination complexes were discovered first and have been extensively studied since.[3] Molecular hybrids can also be used as building blocks for higher dimension objects such as 1D chains, 2D coordination polymers (or networks) as well as 2D and 3D metal-organic frameworks (MOFs).[4] MOFs, also described as porous coordination polymers, are very well described in several reviews.[5-8] Among the different classes of micro/meso-porous materials, MOFs show some advantages, such as their large structural and chemical tunability, allowing to control their pore sizes, shapes and also their selectivity toward strategic gases or vapors, to name a few. They have attracted a lot of attention over the past two decades for a wide range of potential applications.[9-13] Nevertheless, they face several important challenges such as their low electrical conductivity, and sometimes limited chemical, thermal or mechanical stability.

To address these drawbacks, research efforts have focused on different strategies including post synthetic modifications [14, 15], linker functionalization [16-20], inorganic building unit connectivity and dimensionality [21-23], MOFs-based composites etc.[24, 25] Among these latter, MOF/Graphene Oxide(GO) based composites are particularly promising due to the possibility to achieve synergic effects between the porous solid (controlled porosity, selectivity, catalytic activity etc.) and GO (conductivity, light absorption, mechanical stability etc.).

GO is generally obtained from graphite using strong oxidizing agents, based on Hummer's method.[26] The oxygenated groups (mainly hydroxyl and epoxy on the basal plane and carbonyl at the edges) that cover the GO sheets provide interesting possibilities such as covalent or metallic bindings.[27] The chemical reduction or thermal annealing conditions of GO to rGO determine its chemical composition and structure, and therefore properties.[28-32] Respectively, these two graphene derivatives show great promises for various applications.[33, 34] They have been extensively investigated as well as several GO-based composites like noble metals/GO or polymers/GO and their applications that are described elsewhere.[35-37]

MOF/GO and MOF/rGO composites have brought attention for a large range of applications such as CO_2 capture, gas separation, catalysis, supercapacitors etc.[38-48] A few reviews have focused on these systems.[49, 50] For instance, Liu et *al.* reported the syntheses, properties and applications of MOF/carbon-based materials, including the benefits of covalent or non-covalent functionalization of GO and rGO by MOFs.[49] However, to our knowledge, no paper describes the different synthetic approaches used to make such systems or the interactions occurring at the materials' interface which influence the composite properties.

Here, we propose an overview of the different synthetic strategies leading to the formation of composites, ranging from 0D coordination complexes to 3D MOFs coupled with GO or rGO by covalent and non-covalent functionalization as well as the use of MOF/GO as precursors for the formation of metal oxide/rGO composites. We also discuss the challenges related to the characterization of these systems and the need for a better understanding of the mechanisms involved at the materials' interface. Finally, we highlight the importance of the MOF/GO-based composites synthetic strategy on the final material morphology and homogeneity as well as its properties.

II. Coordination complexes/GO (or rGO)

Coordination complexes/GO (rGO) composites have been extensively studied for a wide range of properties related to spintronic[51], sensing[52, 53], catalysis[54-61], energy[62, 63] or medical applications[64], to quote a few. Due to its oxygenated functional groups (hydroxyl, epoxy and carbonyl), GO can bind directly to metal cations.[55] The metal ion is then connected through metallic bonds to the oxygenated groups of GO. Several reports also described the anchoring of chemical species on GO which can coordinate to metal species in a later step.[54, 57, 59, 65-67] The coordination complex is then covalently immobilized on the GO surface. One of the main advantages of these systems in catalysis is that the coordination complex is easily recovered after its use. Also, the grafting of the catalyst on the GO can affect its properties, sometimes leading to an improvement of the activity compared to the parent single complex. When the ligand contains aromatic cycles, it can also interact through $\pi - \pi$ stacking with the basal plane of GO.[61, 62, 68, 69]. Reviews in this field have been published although they are still scarce.[70-73] One can nevertheless consider metal complexes/GO composites as model systems, particularly to

understand the way the metal species interact with the GO when dealing with coordination polymer/GO composites.

III. Coordination polymers/GO (or rGO)

Coordination polymers are 1D, 2D or 3D organic-inorganic hybrid structures.[74-76] MOFs are a sub-class of coordination polymers with 2D or 3D porous architectures.[77] Since MOF/GO and MOF/rGO will be described in the next section, we will focus here on other types of coordination polymers.

Among them, Prussian Blue (PB)/GO (or rGO) composites have been studied to overcome some limitations or to enhance the properties of PB. For instance, it has been shown that the use of GO as a platform for PB immobilization improves the sensor stability (by preventing the PB from aggregating) and activity due to the synergetic effects between PB and GO (or rGO).[78-82] Also, the use of GO allows for an easier recovery of PB that usually requires extensive washing steps. Others reported that PB/GO and PB/rGO systems have a better electrocatalytic activity toward H_2O_2 reduction compared to other reported PB composites or single PB.[79, 81, 82] It was proposed that such a phenomenon was due to the enhanced electron transfer allowed by the GO. Kong *et al*. studied several PB/GO systems with different PB particle sizes for H_2O_2 detection.[82] They managed to obtain PB particles of 5-nm size using an interfacial site-directed growth. More precisely, they added the iron complex very slowly to the GO suspension to promote the interactions between the iron species and the oxygenated groups of GO and therefore to favor the PB nucleation on the GO sheets. They compared the sensitivity toward H_2O_2 between PB simply mixed with GO and the PB/GO composite. Although the authors did not compare the sensitivity limit of the PB/GO systems with PB particles of different sizes, they assigned the observed higher sensitivity obtained with the site-directed growth composite to the very small 5-nm size of their PB particles. The better catalytic results of this composite compared to the PB mixed with GO was assumed to be due to the closer contact between PB particles and GO in the case of very small nanoparticles (Fig 1).

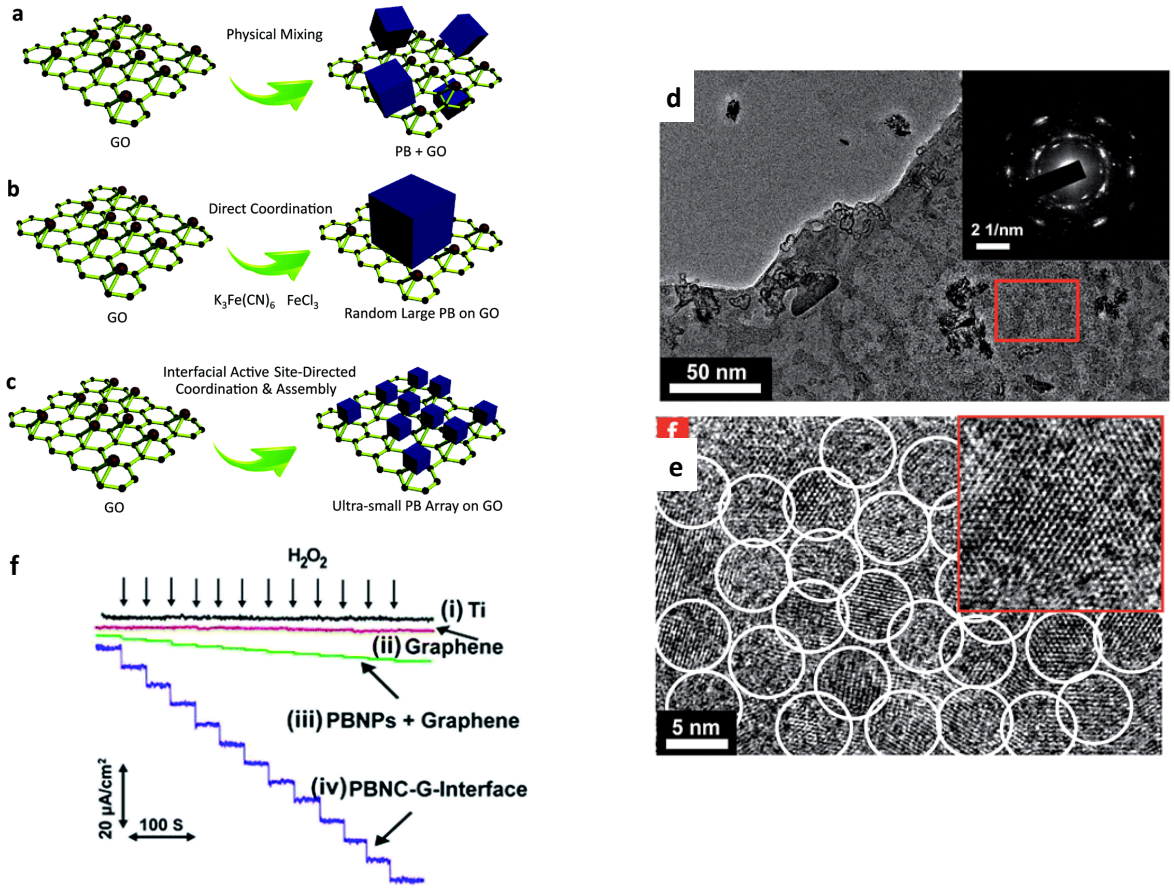

Figure 1. Schematic illustration of PB/GO composites synthesis by a) physical mixing b) direct coordination c) interfacial directed growth d) TEM and e) HRTEM of the PB/GO composite obtained by interfacial directed growth f) Amperometric responses of Ti substrate, graphene, PB nanoparticles mixed with graphene and 5nm PB nanocrystal + graphene. Reprinted with permission from [82]

When dealing with other types of coordination polymers/GO composites, an improvement of the catalytic activity compared to the pristine coordination polymer material was also observed. For instance, a zinc coordination polymer/GO [83] and a cobalt coordination polymer/GO [84] showed better photocatalytic properties towards the reduction of Cr(VI) and the hydrogen evolution reaction (HER), respectively. A few studies also reported the covalent grating of a ruthenium coordination polymer on rGO for photovoltaic applications.[85, 86]

As for coordination complexes, the coordination polymers are either reacted with GO through covalent bindings using the organic linker as connector or through metallic interaction between the metal ions and the oxygenated groups of GO. So far, these systems have mostly been studied for electrochemical applications, taking advantage of the synergetic effects between the two materials.

IV. Synthetic methods of MOF/GO and MOF/rGO

Since the synthetic conditions might strongly impact the nature of the interactions between the MOFs and the GO or rGO and therefore the composite properties, different synthetic strategies have been developed. Generally, the carbon-based starting material is GO. However, it has been shown that the GO undergoes a reduction when the synthesis temperature reaches or exceeds 100 °C.[87, 88] Thus, we will not separate the preparation of MOF/GO composites from MOF/rGO as one may only consider the temperature of the reaction but not the synthetic route.

1. *In Situ*

The *in situ* synthesis route consists of synthesizing the MOF directly in the presence of GO. The most straightforward way is to mix MOF precursors and GO (or rGO) together at ambient temperature, prior to heating the solution under solvothermal or reflux conditions required for the MOF synthesis. Most of reported MOF/GO and MOF/rGO syntheses follow this strategy due to its ease and fast preparation.[38, 40, 42-45, 47, 48, 89-97] C. Petit and T. J. Bandosz were the first to use this procedure to make various MOF/GO composites based on MIL-100, HKUST-1 and MOF-5.[91, 98] The authors found that the oxygenated functional groups of graphite oxide can serve as nucleation points for the MOF. They highlighted the effect of GO over the directional growth of the MOF upon formation of the composites.[99] Because HKUST-1 and MOF-5 possess a cubic structure, these MOFs grow along both the parallel and perpendicular directions compared to the GO sheets. However, in the case of MIL-100, it was not possible to obtain a composite with good crystallinity. This might be due to the more complex chemistry of iron(III)-based MOFs; when growing, the GO sheets can indeed prevent the MOF from forming over a long range distance (Fig 2).

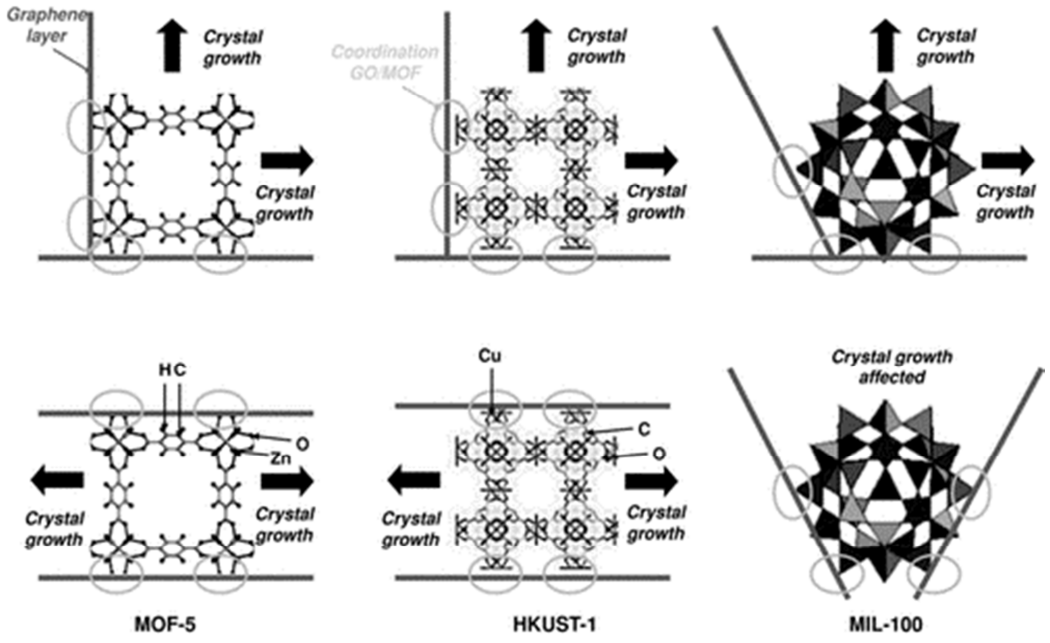

Figure 2. Schematic of the crystal growth of different MOFs, MOF-5, HKUST-1 and MIL-100 on graphite oxide layers. Reprinted with permission from [91]

However, another carboxylate iron-based MOF, MIL-88B(Fe) was successfully anchored on GO using this one-pot synthesis which is likely due to its faster formation kinetics compared to that of MIL-100 (Fe).[100]

Regarding the composites' structural features, it was reported that extra porosity (micro and/or mesoporosity, depending on the MOF) is usually created at the interface of the two materials, enhancing gas adsorption capacity compared to the pure MOF.[38, 40, 42, 48, 97] It appears that the optimal amount of GO for gas sorption depends on the nature of the MOF. In the case of CO_2 capture, the maximum adsorption capacity was reached with only 5 weight% GO for UiO-66[38] while 10 weight% GO was needed in the case of ZIF-8.[101] The creation of extra porosity compared to the parent MOF is associated with the close contact between the two materials as a result of the interactions at the MOF-GO interface.

However, due to binding competition to the metal cation between the GO oxygenated groups and the oxygen atoms of the MOF ligand, the formation of a significant amount of free MOF particles (without GO) can lead to heterogeneous samples. This binding competition can also cause the density of MOF particles decorating the GO sheets to not be optimal, which might decrease the synergy effects between the MOF and GO and therefore the overall performances.

To face this limitation, Qiu *et al*. synthesized MOF/GO composites by reacting the metallic cation with GO prior to the addition of the ligand to the suspension. Theoretically, this method

should promote the direct nucleation of MOF particles on the GO sheets.[102] To highlight the effect of the pretreatment of GO by the metal, the authors compared the one-pot synthesis to this two-steps synthesis on MOF-253(Al) and MIL-101(Cr). Scanning electron microscopy (SEM) images clearly showed that the samples obtained with GO pretreatment have a higher density of MOF particles on the GO sheets, but also bearing a different morphology and size compared to the sample obtained without pretreatment (Fig 3). To better understand the mechanisms of such morphology change, the authors performed Fourier Transformation Infra-Red (FTIR) on the samples with and without pretreatment. For MOF-253, they concluded that aluminum ions mostly interact with the epoxy and hydroxyl moieties of GO. Also, they observed a stronger shift of these oxygen-related bands for the sample in which GO was pretreated for 8 hours by the metal salt compared to the sample without pretreatment. Therefore, the authors suggested that there were more aluminum nuclei for the MOF growth on the pretreated sample. This higher density of nuclei induced some steric hindrance that led to smaller MOF particles with changed morphology. To illustrate the impact of the pretreatment on the composite properties, they performed catalytic tests of ethylbenzene oxidation on samples obtained from pure MIL-101 and the composites with and without pretreatment after pyrolysis at 900 °C. It was observed that not only both composites showed better catalytic activity than the pure MOF, but also that the composite with pretreatment showed the highest activity. The authors attributed this result to the smaller size of particles and therefore more exposed active sites of the pretreated sample in comparison with the two other samples. They also suggested that the higher dispersion of MOF might explain the catalytic results as there are more MOF particles on GO. This example highlights the importance of the reactants order of addition on the structure of the final composite and the impact of the synthesis approach on the final composite morphology and therefore properties. This aspect will be further addressed in the discussion part. Surprisingly, to our knowledge, this is the only study that compares different *in situ* procedures to make MOF/GO composites. Although others reported similar GO pretreatment by metal salts, they did not discuss the benefits of following this synthetic strategy to produce MOF/GO composites.[103-105]

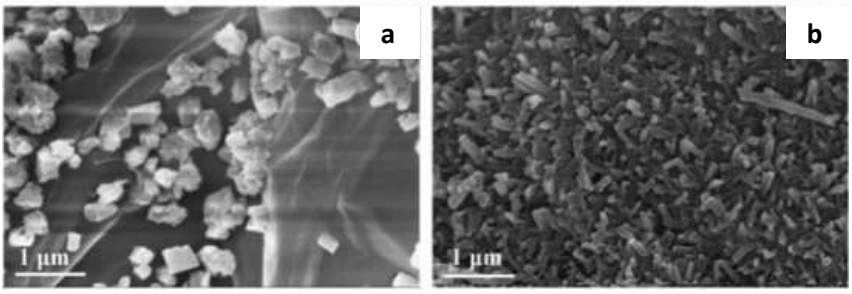

Figure 3. SEM image of MOF-253/GO composites by a) one-pot in situ synthesis b) two steps in situ synthesis using pretreatment of GO by the metal source. Readapted with permission from [102]

Another strategy consists of following a covalent or non-covalent pre-anchoring step of the ligand onto the GO. [41, 106-108]

Jahan *et al.* covalently functionalized GO with a benzoic acid derivative (named BFG) and showed that this pre-anchoring step plays a key role in the MOF growth.[108] They observed that such a functionalization strongly affects the structure of MOF-5 within the composite. The BFG acts as a linker for the MOF and when using 5 weight% BFG, a lattice distortion was observed leading to the formation of nanowires along the [200] axis (Fig 4). The functionalization of GO can thus yield composites with strong interactions between the two materials but can also favor a preferred orientation for the crystal growth. This change in morphology can be of great interest for some applications since it can lead to enhanced or even new properties.[109-111] Different MOF/GO systems were synthesized following this approach and displayed better properties compared to the pure MOF.[41, 112] For instance, after reduction of GO, Lee *et al.* considered the grafting of rGO sheets by azobenzoic acid before the addition of the MOF precursors. They observed some lattice distortions by Powder X-Ray Diffraction (PXRD) and the SEM images revealed a change in the MOF morphology from rectangular to triangular when increasing the GO content.[112] They studied the detection of explosives and found a better sensing response for the composite compared to the parent MOF. However, at this stage it is still not clear how the morphology change affects the MOF's properties and the detailed mechanisms of the template role of GO.

Recently, the synthesis of NH_2-MIL-53/rGO composites using polystyrene (PS) spheres as template for methylene blue photocatalytic degradation was proposed.[113] It was previously shown that hollow spheres have good light absorption properties which can be used for photocatalysis. After wrapping the PS spheres with GO sheets by electrostatic interactions, the GO was further reduced using hydrazine. To ensure the MOF grafting, the rGO was

functionalized by a benzoic acid derivative, prior to the solvothermal synthesis of MOF. To obtain hollow spheres the obtained material was washed with DMF, leading to an efficient removal of the polystyrene.

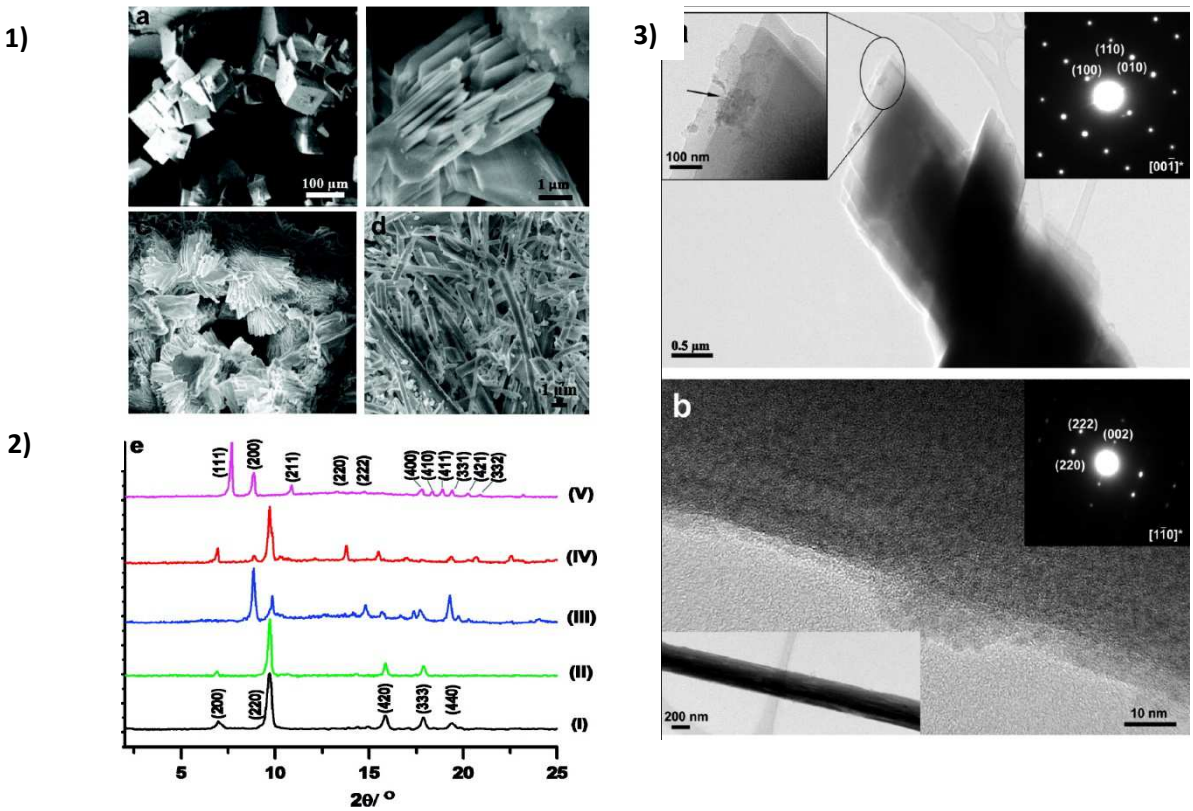

Figure 4. 1) SEM images of a) MOF-5 b) MOF/BFG 1wt% c) MOF/BFG 4wt% d) MOF/BFG 5wt% 2) PXRD patterns of (I) MOF-5 (II) MOF/GO 5wt% (III) MOF/BFG 1wt% (IV) MOF/BFG 4wt% (V) MOF/BFG 5wt% 3) a) TEM images of MOF/BFG 1wt% b) HRTEM of MOF/ BFG 5wt%. Reprinted with permission from [108]. Copyright 2018 American Chemical Society

Other studies described the non-covalent functionalization of GO by the MOF ligand.[106, 107] By introduction of ligands possessing aromatic rings, the large π system of GO allows specific π-π interactions. This template-structure method theoretically leads to minimized distances between the GO sheets and the MOF particles and therefore enhanced interactions. Following this approach, a 'sandwich-like' layered MOF/rGO was obtained using pyrene functionalized GO.[106] The pyrene interacts with GO via π- π interactions and connects the GO and the MOF. The MOF linker was added first to ensure π- π interactions with the pyrene moieties. After addition of the metal source, a solvothermal reaction was carried out to synthesize the MOF. The photocatalytic properties of the composite were studied and compared to the pure MOF and to the composite made without pyrene. A better photo-response was observed for the composite when

using pyrene, which suggests that the sandwich-like structure is partly responsible for the improved catalytic performances.

This non-covalent route appears to lead to different arrangements between the GO and the MOF compared to the covalent one. However, considering that no direct comparison between these two *in situ* procedures is available for a given MOF and GO, the effect of the functionalization method (covalent or not) on the resulting properties is still not well-understood.

2. Post-synthesis

To synthesize MOF/GO composites, a post-synthesis approach has also been reported in the literature.[114, 115] In this case, the GO is directly mixed with the pre-formed MOF at RT. Because GO and MOF surface have different charges, the electrostatic interactions between the two materials lead to self-assembly process.

Recently, Li *et al.* studied the interactions of a family of Zr-MOFs with GO in water at a controlled pH value.[116] By tuning the pH, the MOFs are either positively or negatively charged, and thus cannot interact with the negatively charged GO in the same way. When both materials are oppositely charged, the process is governed by electrostatic interactions. When both have the same surface charge, although electrostatic repulsion occurs, the authors still observed adsorption of GO on the MOFs. They suggested that other types of interaction such as π-π stacking and Lewis acid-base interactions can overcome the electrostatic repulsion. Adsorption of GO on the different MOFs showed that the process is partially irreversible possibly due to a rearrangement of the GO sheets within the composites (Fig 5).

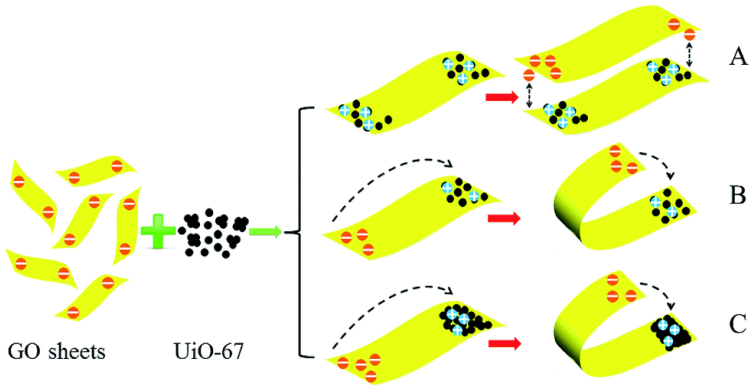

Figure 5. Schematic illustration of possible configurations of aggregation of UiO-67 and GO sheets depending on the materials charge. Reprinted with permission from [116]

Liang *et al.* described two methods for the synthesis of MIL-53(Fe)/rGO. Firstly by mixing the positively charged MOF particles with the negatively charged GO sheets in water, and secondly by mixing the MIL-53(Fe) precursors with GO before using the solvothermal reaction required to produce the MOF.[117] According to Transmission Electron Microscopy (TEM) and X-ray Photoelectron Spectroscopy (XPS) analysis, the sample obtained by electrostatic assembly exhibits a closer contact compared to the *in situ* one. This is likely due to the higher interfacial contact area when a post-synthetic method is used compared to *in situ*; in the case of the post-synthetic method, the MOF appeared to be completely wrapped into the GO whereas the *in situ* synthesis led to random distribution of MOF and GO. The authors also addressed the issue of the presence of free MOF particles that can affect the overall composite properties. Indeed, they observed a better photocatalytic response toward the reduction of Cr(VI) of the post-synthesis sample compared to the *in situ* one with 0.5% rGO. However, the *in situ* composite gave slightly better results with 5% rGO. This change of trend is explained by the presence of additional bare MOF particles contributing to the photocatalytic activity for the *in situ* sample. It suggests that post-synthetic conditions lead, in that case, to more homogeneous composite.

The post-synthetic method is however not commonly used to produce MOF/GO composites. Although the interactions between the two materials are theoretically weaker compared to the direct metallic or covalent bonding in the *in situ* method, mixing the already prepared MOF particles with GO sheets seems to lead to different types of arrangement between the MOF and the GO. Comparison between these two synthesis procedures should give rise to valuable information and therefore needs further investigation.

3. Other routes

In addition to the *in situ* and post-synthesis strategies, less common methods have been proposed to synthesize MOF/GO composites. Bian *et al.* described the synthesis of $Cu_3(BTC)_2$/GO by pickering emulsion.[118] The large interfacial area of droplets allows to optimize the surface contact between the two materials compared to direct MOF growth on bulk GO. As a proof of concept they compared the CO_2 uptake under humid conditions of the $Cu_3(BTC)_2$/GO obtained by pickering emulsion and the one obtained by simply mixing $Cu_3(BTC)_2$ with GO. GO sheets are better exfoliated using the emulsion method and therefore have stronger affinities for water compared to bulk GO (Fig 6). Due to this affinity, the water molecules are preferentially

adsorbed on GO instead of the MOF pores. However, for the post-synthesis sample, both CO_2 and H_2O are adsorbed by the MOF. Therefore, the post-synthesis sample gave lower CO_2 uptake under humid conditions compared to the emulsion sample. Zhang *et al.* also used the same emulsion approach to synthesize Zr-BDC-NO_2/GO composites.[119]

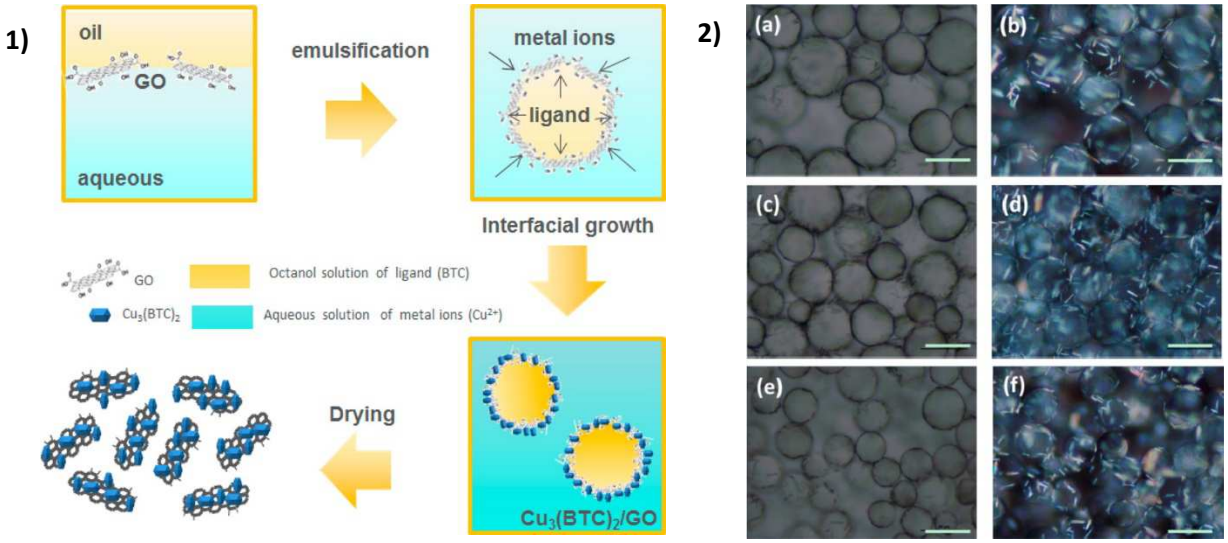

Figure 6. 1) Schematic illustration of the emulsion synthesis of $Cu_3(BTC)_2$/GO composite 2) a)c)e) Optical micrographs and b)d)f) polarized optical micrographs of $Cu_3(BTC)_2$/GO composite with different GO amount. Reprinted with permission from [118] Copyright 2018 American Chemical Society

To ensure covalent interactions between the MOF and GO, Meng *et al.* used the carmodiimide, named EDC, to form amide bonds between the carboxylic acid groups of GO and the amine moieties of the MOF ligand.[120] After mixing the GO sheets with the coupling agent EDC, they added the pre-formed MIL-88B-NH_2 and MIL-101-NH_2. The two MOF/GO systems were studied for photodynamic therapy. Interestingly, after coupling these two MOFs with GO, it was observed that the stability in water was enhanced compared to the parent MOFs. Indeed, because the pure MOFs exhibit both a positive zeta-potential at low pH, their stability in water is limited when the pH increases. However, for the composites, negative zeta-potential values were measured, explaining the longer time stability in water of these MOF/GO systems.

V. Thermal treatment of MOF/GO composites

Pure MOFs, as an ideal source of spatially controlled inorganic moieties embedded into an organic ligand environment, have already been studied as starting compounds to produce various types of materials through carbonization.[121] After their pyrolysis, a large variety of structures, for instance, metal or metal oxide (or nitride) nanoparticles can be obtained.[122] The same

concept can be applied to MOF/GO composites. Their thermal treatment under oxygen rich atmosphere can for instance, lead to metal oxide/rGO composites. Kim *et al*. studied the effect of the annealing temperatures (250, 450 and 650 °C) on the particle size, CO_2 uptake and electric conductivity of ZIF-8/rGO composites.[103] They showed that the thermal treatment of ZIF-8/GO involves the creation of additional mesopores that can be tuned with the calcination temperature. As expected, the higher the temperature the higher the conductivity due to an increase of GO reduction (Fig 7).

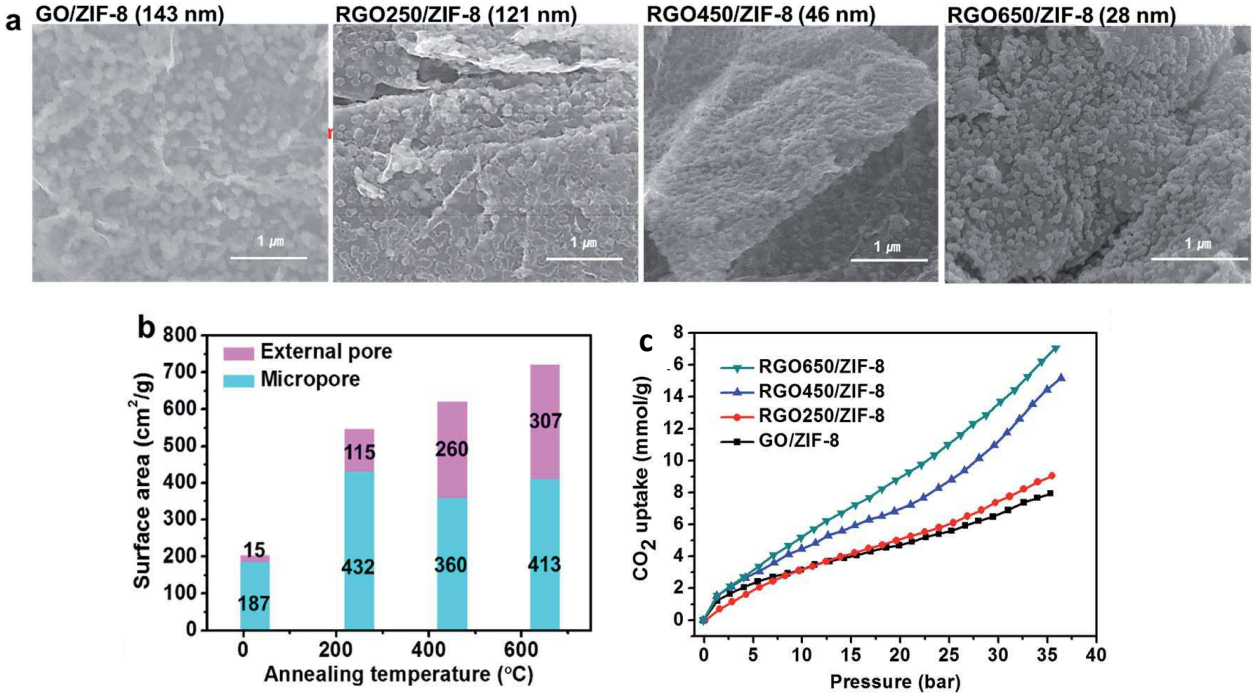

Figure 7. a) SEM images b) BET surface area and c) CO_2 uptake isotherms of ZIG-8/GO and the corresponding composites after calcination at 250, 450 and 650 °C. Reprinted with permission from [103]

The microwave absorption properties of the composites obtained from MOF/GO annealing have also been assessed.[105, 123] The response of the material to electromagnetic waves is described by its permittivity and permeability. The permittivity loss ε", *i.e.* the ability of a material to convert the absorbed energy, increases after reduction due to the presence of conductive rGO that increases the conduction loss. However, high permittivity and permeability losses do not automatically lead to good electromagnetic absorption properties. Indeed, it also requires a very good impedance matching, hence close complex permittivity and complex permeability values.[124] Therefore, the annealing temperature of MOF/GO composites for electromagnetic absorption must be chosen depending on these parameters. Although the mechanisms responsible

for such electromagnetic wave response are not very well understood, MOF/GO derived composites seem to offer a good alternative as microwave absorber materials.

These carbonized composites also raised a significant interest for electrochemical applications. Due to the thermal reduction of the insulating GO to the conductive rGO, MOF-derived metal oxide/rGO composites have been reported as interesting battery materials.[65, 125-127] The electrical conductivity of rGO can indeed overcome the poor electrical conductivity of metal oxides and also improve the mechanical stability of the material. The use of MOFs as a self-sacrificing template for metal oxide is also believed to enhance the particles dispersion on GO and therefore maximize the reachability of the active sites. The better performances for Li-ion batteries of Co_3O_4/rGO obtained from ZIF-67(Co)/GO compared to pure Co_3O_4 and Co_3O_4/rGO obtained by direct deposition of the cobalt oxide on GO sheets was reported.[127] In addition to the good conductivity of rGO, the authors attributed these results to the well-dispersed small nanoparticles resulting from the calcination of ZIF-67 as well as shorter diffusion paths for ions.

Although most of the reported procedures described the first step of the synthesis as the production of MOF/GO composite prior to its thermal treatment, other routes can be found in the literature. For instance, the annealing of the MOF before its electrostatic reaction with GO was described.[128] Cao *et al.* used a post-synthesis procedure to obtain Mo-MOF wrapped into GO sheets. After annealing, the rGO-wrapped MoO_3 material showed a better supercapacitor performance compared to pure MoO_3.[129]

Due to the intrinsic conductive behavior of rGO and the exposed active metal sites of MOFs, MOF/GO composites have also been studied as precursors for electrocatalysis.[95, 130-134] They might offer a good alternative compared to expensive Pt-based materials for hydrogen evolution reaction (HER), oxygen evolution reaction (OER) and oxygen reduction reaction (ORR).[95, 135] MOF-74(Ni) appears particularly interesting for HER and OER due to the possibility of forming nickel sulfide or nickel phosphide after pyrolysis.[130, 131] Based on previous works [134, 136] Wei *et al.* studied the performances of ZIF-67/GO based composites for ORR applications.[137] To highlight the importance of the MOF distribution on the GO sheets over the composite properties, the authors compared the direct deposition of ZIF-67 on GO and the use of ZIF-8 seeds for the growth of ZIF-67 on GO as precursors for the preparation of cobalt nanoparticles/carbon-based composites. In agreement with previous reports,[136, 138] they observed that direct growth of ZIF-67 on GO sheets led to larger crystals (around 80 nm)

and inhomogeneous MOF distribution on GO sheets. However, when using ZIF-8 grafted GO as seeds for ZIF-67 growth, much smaller particles were produced. After thermal treatment at 900 °C, the core-shell structure showed better catalytic performances compared to the materials obtained from ZIF-8/GO and ZIF-67/GO precursors, mostly due to a higher coverage density of MOF (and therefore cobalt active sites after annealing) (Fig 8).

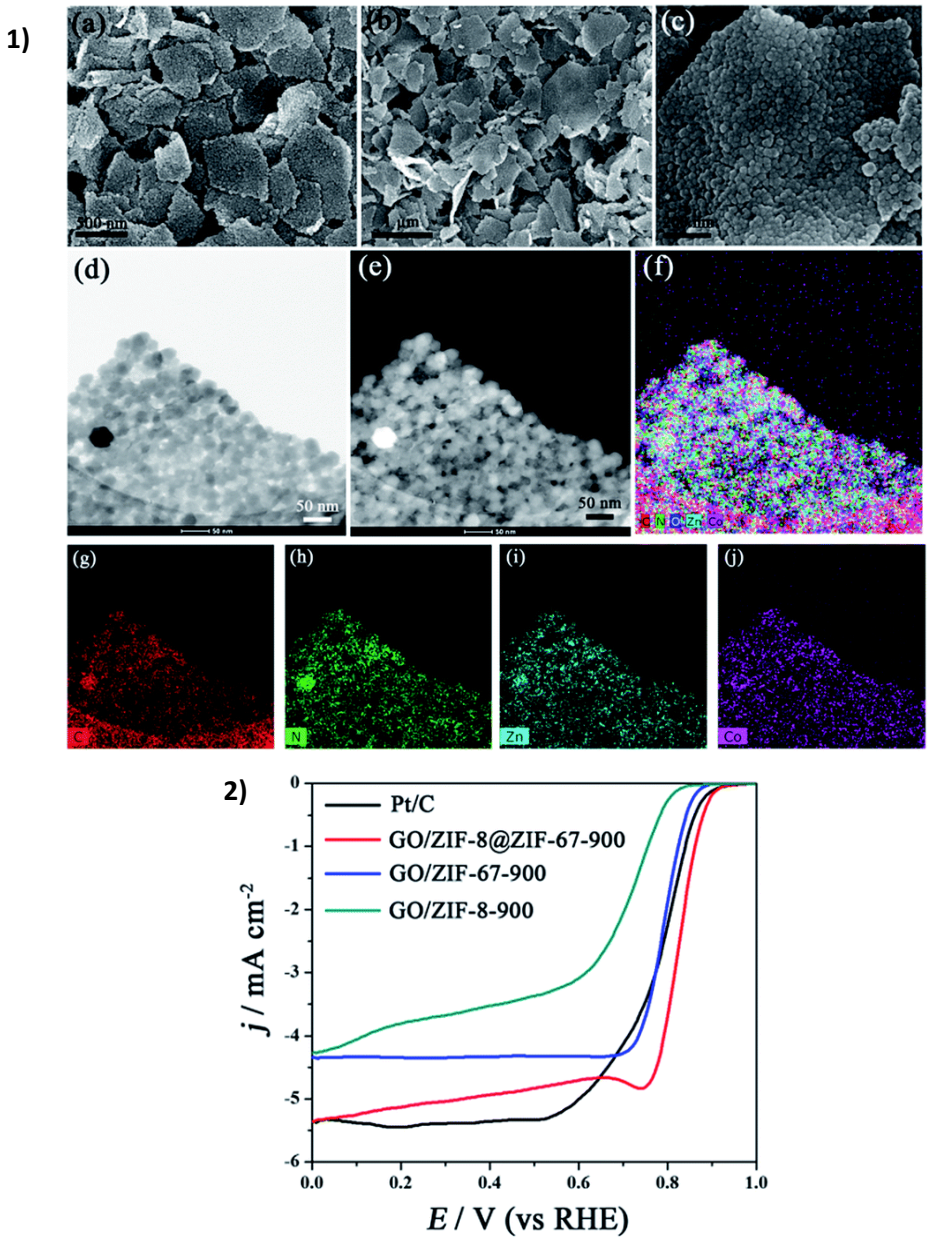

Figure 8. 1) SEM images of a) ZIF-8/GO b)c) ZIF-8@ZIF-67/GO d-j) TEM and corresponding mapping of ZIF-8@ZIF-67/GO 2) Linear sweep voltammetry curves of Pt/C, ZIF-8/GO, ZIF-67GO and ZIF-8@ZIF-67/GO calcinated at 900 °C. Reprinted with permission from [137]

The effect of core-shell structure on the catalytic properties of Co-based MOFs was also reported.[139] It was shown that the presence of metal oxide between the metal and rGO could increase the generation of hydrogen from $NaBH_4$ due to enhanced synergistic effects at the interfaces.

The synthesis of porous carbon materials have brought lots of attention and efforts.[140] MOFs can be used as templates to create additional porosity within GO. It was reported that the controlled carbonization of ZIF-8 can lead to a narrow distribution of mesopores for the GO envelope.[141]

VI. Discussion

GO and rGO have attracted considerable attention in the past decades. However, as promising as these materials are in terms of potential applications, their in-depth characterization is not trivial. GO itself was discovered in 1859 by Brodie[142], but it is only at the beginning of the 21st century that this 2D material gained more interest from researchers. In 2007, Stankovich *et al*. proposed its chemical reduction using hydrazine.[143] The structure determination of GO and rGO was possible only through the use of advanced characterization techniques such as high-resolution XPS [144] and high-resolution TEM.[27, 145]

Therefore, if one considers that MOFs are (i) rather fragile materials, sensitive to a fast degradation under beam irradiation and (ii) composed of a large amount of organic components, this makes it even more challenging to fully characterize the MOF/GO and MOF/rGO composites compared to pure GO (or rGO). Indeed, in most cases, usual techniques such as powder X-ray diffraction, infra-red spectroscopy, electron microscopies and thermogravimetric analysis (TGA) only confirm that the MOF structure is kept within the composite. In some cases, PXRD pattern of the composites can nevertheless show the characteristic peak of GO or rGO, slightly shifted, suggesting some different interlayer distances caused by the MOF intercalation between the sheets.[104, 119] If considering TGA, special care must be taken for MOF/GO composites. It is well known that upon heating, CO_2 and CO are released from GO. The resulting thermal expansion leads to a strong mass loss around 200 °C.[143] However, this loss is due to the expulsion of material during the explosive exfoliation. Therefore, TGA of MOF/GO composites should not be operated at a high heating rate (above 5 °C/min) under oxygen atmosphere to provide reliable results. In addition, so far most of the reported composites were made using a

low GO (or rGO) quantity; thus the resolution limit of TGA must be taken into account when characterizing composites built up from less than 10 wt% GO.

Nitrogen porosimetry is a well-established and powerful tool to characterize porous solids. Petit *et al.* were the first to observe an increase of the BET surface area of MOF-5/GO10% compared to the parent MOF-5. It was suggested that this increase is due to the creation of extra porosity at the materials' interface.[98] The creation of extra porosity suggests a very close contact between the MOF and the GO sheets. The amount of GO that leads to maximum adsorption depends on the system. Generally, it appears that 10wt% GO content leads to the highest nitrogen uptake. Above 10wt%, further addition of this porous material with low porosity usually leads to a decrease in the BET surface area. Also, GO can partially block the MOF porosity, especially for microporous MOFs. This phenomena was observed for MIL-125(Ti) with 10% GO.[146] The surface area of the composite is almost 60% lower than the one of the pure MOF.

Electron microscopies (SEM and TEM) give information on the arrangement (wrapping, intercalation etc.) between the MOF and the GO. The mapping of elements using high-resolution TEM also gives information on the MOF dispersion as well as the sample homogeneity. However, to our knowledge the presence of single components, *i.e.* free MOF particles (without GO) or free GO nanosheets (without MOF) is seldom addressed although the composite homogeneity might impact its properties.

The effect of GO or rGO on MOF crystals was also studied by electron microscopy. It is very interesting to note that for *in situ* syntheses, GO can strongly impact the size and shape of the MOF particles within the composite or even prevent its formation in some cases.[40, 95, 99, 101] It was suggested that because of the interactions between the oxygenated groups of GO and the metal centers from the MOF, the growth of MOF particles can be somehow inhibited. Therefore, in presence of GO, smaller MOF particles are often observed compared to the pure parent material particularly when the GO content increases. Also, it was shown that one can tailor the MOF's morphology by selecting the right composite synthetic method. Indeed, it appears that GO can act as a template for the MOF either directly by functionalization of its surface or indirectly by providing dense and close nucleation sites for the MOF growth. This is of great interest considering that the size and shape often strongly affect the final properties. By monitoring these structural features, new and/or enhanced properties can emerge.

Raman spectroscopy is another tool to characterize graphene and its derivatives,[147, 148] and thus MOF/GO composites. However, there are still some debates about the use of Raman for GO. Generally, the ratio of the D band over the G band intensity is used to quantify the amount of defects. However, a few papers highlighted that these two bands consist in fact of a superimposition of several bands. Therefore, the intensity ratio cannot be directly used to estimate the disorder degree and therefore the functionalization of GO (Fig 9). [149, 150]

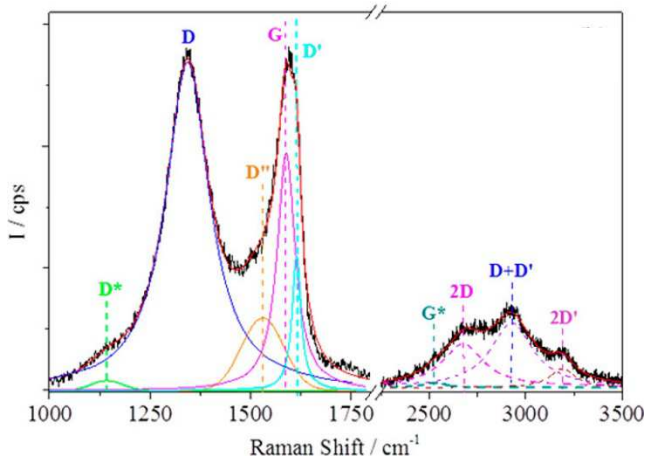

Figure 9. Deconvolution of the Raman spectra of graphene oxide obtained by oxidation of pyrolytic graphite. Reprinted with permission from [150] Copyright 2018 American Chemical Society

Among all characterizations reported for MOF/GO, high-resolution XPS appears to be a very appropriate technique to analyze the interactions between these two materials, particularly to determine which oxygen group (carboxyl, hydroxyl etc.) is involved.[151]. Indeed, a shift of the bands (metal, oxygen) compared to those of the pure MOF or pure GO can be observed (Fig 10).[89, 106] This shift shows that the local electronic environment of one material is affected by the other, giving proofs of covalent or non-covalent interactions between the MOF and the GO. Therefore, XPS not only gives information about the nature of the interactions between the materials but also about which specific atoms are involved. Also, XPS can be used as a probe to assess the degree of homogeneity of the composite.

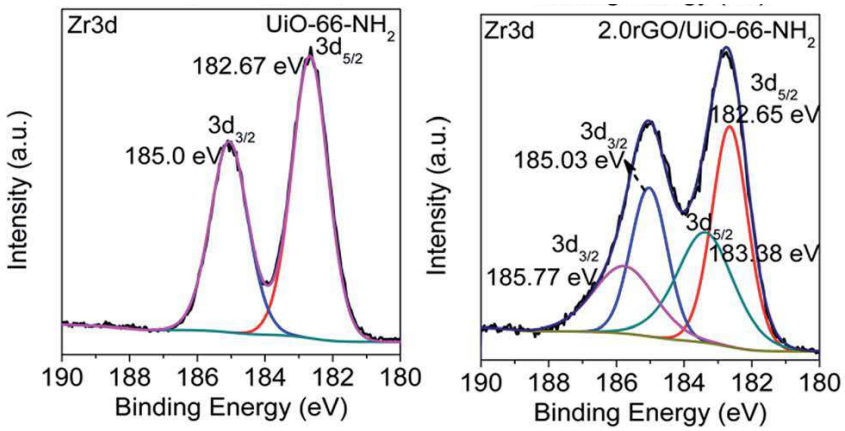

Figure 10. Zr3d XPS spectra of UiO-66-NH_2 and UiO-66-NH_2/rGO2%. Reprinted with permission from [106]

Surprisingly, no solid-state NMR study was reported for MOF/GO composites so far. Although, ^{13}C solid-state NMR was previously used to characterize the structure of bare GO which shed light on the nature of oxygen groups at the GO surface.[152, 153] One possible explanation could be the very low content of NMR nuclei (H, C) at the MOF-GO interface which certainly makes the NMR analysis much more challenging. One possibility to overcome this issue would be to consider Dynamic Nuclear Polarization (DNP) to provide meaningful information on the MOF-GO interface. This technique can lead, through the use of radicals that diffuse within the pores, to a spectacular enhancement of the signal to noise ratio of the NMR signals.[154, 155] Another way to boost the sensitivity of the NMR spectra would be to enrich the composite with ^{13}C or ^{17}O species, as done recently for MOF characterization.[156, 157]

By combining several characterization techniques, useful information regarding the nature of interactions involved, size, shape, arrangement etc. of particles can be obtained. However, there is still a lack of understanding regarding (i) the impact of the GO or rGO dispersion on the structure of the composite (ii) the GO quantification within the composite.

When GO is produced from graphite, the exfoliation method and duration, as well as its concentration strongly affect its dispersion. Among the reports on MOF/GO synthesis, several derivatives of the Hummer's method were used, leading to different GO dispersions (and degree of oxidation). It was reported that the electrostatic repulsion between the GO sheets and intercalation of water molecules enables to obtain well-dispersed colloidal suspension of GO monolayers in aqueous media.[143, 158] However, as several exfoliation methods to produce GO exist, we believe that the dispersion quality might seriously affect the arrangement of the MOF and GO particles. Also, the reduction of GO to rGO leads to a less hydrophilic material that can

easily agglomerate in water.[159] The degree of exfoliation of GO or rGO is thus an important parameter to consider when producing MOF/GO composites. This is even more important when considering a non-aqueous synthetic medium as it was shown that GO can take on different shapes, more or less compact, by self-assembly depending on the treatment method.[160, 161]
Also, as synthetic procedures usually describe the addition of an average weight percentage of GO compared to the pure MOF, considering that the MOF yield might change due to the presence of GO, the theoretical content of GO is probably slightly different from the experimental one. In addition, as the GO content within the composites is generally low, a precise quantification would require a combination of very sensitive advanced characterization methods.

VII. Conclusion

The development of advanced organic-inorganic hybrid materials/GO-based composites with promising properties has made significant progress over the past few years. From the smaller unit *i.e* 1D coordination complexes to 3D MOFs, the addition of graphene oxide can indeed improve several properties compared to the bare hybrid material. This has been particularly demonstrated for MOFs. Indeed, MOF/GO composites can show enhanced gas adsorption, mechanical and chemical stability, conductivity etc.. These final composite properties can be easily tailored by varying the synthetic approach. It has been shown that the synthetic conditions not only affect the nature of interactions between the two materials, but also the MOF particle size, shape, homogeneity and distribution density on GO. This is of great interest as properties often depend on the MOF morphology. These composites can also be used as precursors to prepare various types of materials, depending on the reduction temperature and method. Therefore, MOF/GO-based composites appear as a versatile platform associated with enhanced properties compared to the pure materials. However, their precise characterization, particularly at the microscopic level, remains challenging. Recently, few examples have demonstrated that combining advanced experimental characterization and modelling tools can give a better understanding of the materials' interface microstructures. For instance, the ZIF-8/GO interface was described.[162] The authors shed light through DTF and force-field-based molecular dynamics calculations, on the nature of interactions between MOF and GO and where MOF distribution is favored on GO. They showed that ZIF-8 and GO have a good affinity and were able to predicted the trends in

tensile strength of their composites. Their simulations were then confirmed by experimental studies. We believe that, in the near future, it will be possible to predict the suitability of a synthetic approach to reach a specific property and to understand the mechanisms that improve or create new properties compared to the parent materials. Considering the large number of existing hybrid species, as well as the tunability of GO surface, it is likely that this field has a broad potential that demands further investigations.

Acknowledgement

This work was supported by the European project H2020 Gramofon (727619). The authors acknowledge Sarah McKinney for her valuable help in revising the manuscript.

[1] P. Judeinstein, C. Sanchez, Journal of Materials Chemistry, 6 (1996) 511-525.
[2] A.K. Cheetham, C.N.R. Rao, R.K. Feller, Chemical Communications, (2006) 4780-4795.
[3] W.C. Zeise, Ann. Phys. Chem., 6 (1827) 632.
[4] C. Janiak, J.K. Vieth, New Journal of Chemistry, 34 (2010) 2366-2388.
[5] S.L. James, Chemical Society Reviews, 32 (2003) 276-288.
[6] A.J. Howarth, A.W. Peters, N.A. Vermeulen, T.C. Wang, J.T. Hupp, O.K. Farha, Chemistry of Materials, 29 (2017) 26-39.
[7] A. Kirchon, L. Feng, H.F. Drake, E.A. Joseph, H.-C. Zhou, Chemical Society Reviews, (2018) 8611-8638.
[8] A. Schneemann, V. Bon, I. Schwedler, I. Senkovska, S. Kaskel, R.A. Fischer, Chemical Society Reviews, 43 (2014) 6062-6096.
[9] H. Furukawa, K.E. Cordova, M. O'Keeffe, O.M. Yaghi, Science, 341 (2013) 1230444.
[10] M. Giménez-Marqués, T. Hidalgo, C. Serre, P. Horcajada, Coordination Chemistry Reviews, 307 (2016) 342-360.
[11] W.P. Lustig, S. Mukherjee, N.D. Rudd, A.V. Desai, J. Li, S.K. Ghosh, Chemical Society Reviews, 46 (2017) 3242-3285.
[12] L. Zhu, X.-Q. Liu, H.-L. Jiang, L.-B. Sun, Chemical Reviews, 117 (2017) 8129-8176.
[13] K. Adil, Y. Belmabkhout, R.S. Pillai, A. Cadiau, P.M. Bhatt, A.H. Assen, G. Maurin, M. Eddaoudi, Chemical Society Reviews, 46 (2017) 3402-3430.
[14] Z. Wang, S.M. Cohen, Chemical Society Reviews, 38 (2009) 1315-1329.
[15] Y. Ye, W. Guo, L. Wang, Z. Li, Z. Song, J. Chen, Z. Zhang, S. Xiang, B. Chen, Journal of the American Chemical Society, 139 (2017) 15604-15607.
[16] M. Kandiah, M.H. Nilsen, S. Usseglio, S. Jakobsen, U. Olsbye, M. Tilset, C. Larabi, E.A. Quadrelli, F. Bonino, K.P. Lillerud, Chemistry of Materials, 22 (2010) 6632-6640.
[17] S. Biswas, T. Ahnfeldt, N. Stock, Inorganic Chemistry, 50 (2011) 9518-9526.
[18] J.L.C. Rowsell, O.M. Yaghi, Journal of the American Chemical Society, 128 (2006) 1304-1315.
[19] T. Devic, P. Horcajada, C. Serre, F. Salles, G. Maurin, B. Moulin, D. Heurtaux, G. Clet, A. Vimont, J.-M. Grenèche, B.L. Ouay, F. Moreau, E. Magnier, Y. Filinchuk, J. Marrot, J.-C. Lavalley, M. Daturi, G. Férey, Journal of the American Chemical Society, 132 (2010) 1127-1136.
[20] L.N. McHugh, M.J. McPherson, L.J. McCormick, S.A. Morris, P.S. Wheatley, S.J. Teat, D. McKay, D.M. Dawson, C.E.F. Sansome, S.E. Ashbrook, C.A. Stone, M.W. Smith, R.E. Morris, Nature Chemistry, 10 (2018) 1096-1102.
[21] H. Wu, T. Yildirim, W. Zhou, The Journal of Physical Chemistry Letters, 4 (2013) 925-930.
[22] V. Guillerm, F. Ragon, M. Dan-Hardi, T. Devic, M. Vishnuvarthan, B. Campo, A. Vimont, G. Clet, Q. Yang, G. Maurin, G. Férey, A. Vittadini, S. Gross, C. Serre, Angewandte Chemie International Edition, 51 (2012) 9267-9271.
[23] D. Bradshaw, A. Garai, J. Huo, Chemical Society Reviews, 41 (2012) 2344-2381.
[24] Q.-L. Zhu, Q. Xu, Chemical Society Reviews, 43 (2014) 5468-5512.
[25] S. Li, F. Huo, Nanoscale, 7 (2015) 7482-7501.
[26] W.S. Hummers, R.E. Offeman, Journal of the American Chemical Society, 80 (1958) 1339-1339.
[27] K. Erickson, R. Erni, Z. Lee, N. Alem, W. Gannett, A. Zettl, Advanced Materials, 22 (2010) 4467-4472.
[28] G. Eda, C. Mattevi, H. Yamaguchi, H. Kim, M. Chhowalla, The Journal of Physical Chemistry C, 113 (2009) 15768-15771.
[29] C. Mattevi, G. Eda, S. Agnoli, S. Miller, K.A. Mkhoyan, O. Celik, D. Mastrogiovanni, G. Granozzi, E. Garfunkel, M. Chhowalla, Advanced Functional Materials, 19 (2009) 2577-2583.
[30] K.P. Loh, Q. Bao, G. Eda, M. Chhowalla, Nat Chem, 2 (2010) 1015-1024.
[31] I. Jung, D.A. Dikin, R.D. Piner, R.S. Ruoff, Nano Letters, 8 (2008) 4283-4287.
[32] S. Pei, H.-M. Cheng, Carbon, 50 (2012) 3210-3228.
[33] G. Eda, M. Chhowalla, Advanced Materials, 22 (2010) 2392-2415.

[34] M. Nurunnabi, K. Parvez, M. Nafiujjaman, V. Revuri, H.A. Khan, X. Feng, Y.-k. Lee, RSC Advances, 5 (2015) 42141-42161.
[35] X. Huang, X. Qi, F. Boey, H. Zhang, Chemical Society Reviews, 41 (2012) 666-686.
[36] X. Gong, G. Liu, Y. Li, D.Y.W. Yu, W.Y. Teoh, Chemistry of Materials, 28 (2016) 8082-8118.
[37] V. Georgakilas, J.N. Tiwari, K.C. Kemp, J.A. Perman, A.B. Bourlinos, K.S. Kim, R. Zboril, Chemical Reviews, 116 (2016) 5464-5519.
[38] Y. Cao, Y. Zhao, Z. Lv, F. Song, Q. Zhong, Journal of Industrial and Engineering Chemistry, 27 (2015) 102-107.
[39] O. Fleker, A. Borenstein, R. Lavi, L. Benisvy, S. Ruthstein, D. Aurbach, Langmuir, 32 (2016) 4935-4944.
[40] R. Kumar, K. Jayaramulu, T.K. Maji, C.N.R. Rao, Chemical Communications, 49 (2013) 4947-4949.
[41] R. Kumar, D. Raut, U. Ramamurty, C.N.R. Rao, Angewandte Chemie International Edition, 55 (2016) 7857-7861.
[42] S. Liu, L. Sun, F. Xu, J. Zhang, C. Jiao, F. Li, Z. Li, S. Wang, Z. Wang, X. Jiang, H. Zhou, L. Yang, C. Schick, Energy & Environmental Science, 6 (2013) 818-823.
[43] Y. Shen, Z. Li, L. Wang, Y. Ye, Q. Liu, X. Ma, Q. Chen, Z. Zhang, S. Xiang, Journal of Materials Chemistry A, 3 (2015) 593-599.
[44] N.A. Travlou, K. Singh, E. Rodriguez-Castellon, T.J. Bandosz, Journal of Materials Chemistry A, 3 (2015) 11417-11429.
[45] Y. Wang, W. Zhang, X. Wu, C. Luo, T. Liang, G. Yan, Journal of Magnetism and Magnetic Materials, 416 (2016) 226-230.
[46] X. Xu, W. Shi, P. Li, S. Ye, C. Ye, H. Ye, T. Lu, A. Zheng, J. Zhu, L. Xu, M. Zhong, X. Cao, Chemistry of Materials, 29 (2017) 6058-6065.
[47] Y. Zhang, G. Li, H. Lu, Q. Lv, Z. Sun, RSC Advances, 4 (2014) 7594-7600.
[48] X. Zhou, W. Huang, J. Liu, H. Wang, Z. Li, Chemical Engineering Science, 167 (2017) 98-104.
[49] X.-W. Liu, T.-J. Sun, J.-L. Hu, S.-D. Wang, Journal of Materials Chemistry A, 4 (2016) 3584-3616.
[50] Y. Zheng, S. Zheng, H. Xue, H. Pang, Advanced Functional Materials, 28 (2018) 1804950.
[51] Y. Murashima, M.R. Karim, N. Saigo, H. Takehira, R. Ohtani, M. Nakamura, M. Koinuma, L.F. Lindoy, K. Kuroiwa, S. Hayami, Inorganic Chemistry Frontiers, 2 (2015) 886-892.
[52] H. Li, F. Liu, S. Sun, J. Wang, Z. Li, D. Mu, B. Qiao, X. Peng, Journal of Materials Chemistry B, 1 (2013) 4146-4151.
[53] Y. Yu, M. Zhou, W. Shen, H. Zhang, Q. Cao, H. Cui, Carbon, 50 (2012) 2539-2545.
[54] X. Zhou, T. Zhang, C.W. Abney, Z. Li, W. Lin, ACS Applied Materials & Interfaces, 6 (2014) 18475-18479.
[55] Y. Dong, J. Li, L. Shi, J. Xu, X. Wang, Z. Guo, W. Liu, Journal of Materials Chemistry A, 1 (2013) 644-650.
[56] X. Li, Z. Hao, F. Zhang, H. Li, ACS Applied Materials & Interfaces, 8 (2016) 12141-12148.
[57] Q. Zhao, D. Chen, Y. Li, G. Zhang, F. Zhang, X. Fan, Nanoscale, 5 (2013) 882-885.
[58] J. Han, Y.J. Sa, Y. Shim, M. Choi, N. Park, S.H. Joo, S. Park, Angewandte Chemie International Edition, 54 (2015) 12622-12626.
[59] Q. Zhao, Y. Li, R. Liu, A. Chen, G. Zhang, F. Zhang, X. Fan, Journal of Materials Chemistry A, 1 (2013) 15039-15045.
[60] M. Latorre-Sánchez, C. Lavorato, M. Puche, V. Fornés, R. Molinari, H. Garcia, Chemistry – A European Journal, 18 (2012) 16774-16783.
[61] S. Sabater, J.A. Mata, E. Peris, ACS Catalysis, 4 (2014) 2038-2047.
[62] T.-T. Meng, Z.-B. Zheng, K.-Z. Wang, Langmuir, 29 (2013) 14314-14320.
[63] Z. Wang, H. Yao, F. Zhang, W. Li, Y. Yang, X. Lu, Journal of Materials Chemistry A, 4 (2016) 16476-16483.
[64] Z. Ma, B. Moulton, Coordination Chemistry Reviews, 255 (2011) 1623-1641.

[65] Z. Li, C. Li, X. Ge, J. Ma, Z. Zhang, Q. Li, C. Wang, L. Yin, Nano Energy, 23 (2016) 15-26.
[66] H. Su, Z. Li, Q. Huo, J. Guan, Q. Kan, RSC Advances, 4 (2014) 9990-9996.
[67] R.H. Fath, S.J. Hoseini, H.G. Khozestan, Journal of Organometallic Chemistry, 842 (2017) 1-8.
[68] J.N. Lekitima, K.I. Ozoemena, C.J. Jafta, N. Kobayashi, Y. Song, D. Tong, S. Chen, M. Oyama, Journal of Materials Chemistry A, 1 (2013) 2821-2826.
[69] M. Zhu, Y. Dong, B. Xiao, Y. Du, P. Yang, X. Wang, Journal of Materials Chemistry, 22 (2012) 23773-23779.
[70] J. Xu, Y. Wang, S. Hu, Microchimica Acta, 184 (2017) 1-44.
[71] M.R. Axet, O. Dechy-Cabaret, J. Durand, M. Gouygou, P. Serp, Coordination Chemistry Reviews, 308 (2016) 236-345.
[72] S. Zheng, H. Xue, H. Pang, Coordination Chemistry Reviews, (2017).
[73] E. Perez-Mayoral, V. Calvino-Casilda, E. Soriano, Catalysis Science & Technology, 6 (2016) 1265-1291.
[74] C. Janiak, Dalton Transactions, (2003) 2781-2804.
[75] W. Lin, W.J. Rieter, K.M.L. Taylor, Angewandte Chemie International Edition, 48 (2009) 650-658.
[76] S. Kitagawa, R. Matsuda, Coordination Chemistry Reviews, 251 (2007) 2490-2509.
[77] S. Batten, N. Champness, X.-M. Chen, J. García-Martínez, S. Kitagawa, L. Öhrström, M. O Keeffe, M. Suh, J. Reedijk, Terminology of metal–organic frameworks and coordination polymers (IUPAC Recommendations 2013)*, 2013.
[78] B. Kong, C. Selomulya, G. Zheng, D. Zhao, Chemical Society Reviews, 44 (2015) 7997-8018.
[79] Y. Zhang, X. Sun, L. Zhu, H. Shen, N. Jia, Electrochimica Acta, 56 (2011) 1239-1245.
[80] H. Yang, L. Sun, J. Zhai, H. Li, Y. Zhao, H. Yu, Journal of Materials Chemistry A, 2 (2014) 326-332.
[81] L. Cao, Y. Liu, B. Zhang, L. Lu, ACS Applied Materials & Interfaces, 2 (2010) 2339-2346.
[82] B. Kong, X. Sun, C. Selomulya, J. Tang, G. Zheng, Y. Wang, D. Zhao, Chemical Science, 6 (2015) 4029-4034.
[83] G.-M. Shi, B. Zhang, X.-X. Xu, Y.-H. Fu, Dalton Transactions, 44 (2015) 11155-11164.
[84] J. Balapanuru, G. Chiu, C. Su, N. Zhou, Z. Hai, Q.-h. Xu, K.P. Loh, ACS Applied Materials & Interfaces, 7 (2015) 880-886.
[85] R. Vinoth, S.G. Babu, V. Bharti, V. Gupta, M. Navaneethan, S.V. Bhat, C. Muthamizhchelvan, P.C. Ramamurthy, C. Sharma, D.K. Aswal, Y. Hayakawa, B. Neppolian, Scientific Reports, 7 (2017) 43133.
[86] Z. Fang, A. Ito, A.C. Stuart, H. Luo, Z. Chen, K. Vinodgopal, W. You, T.J. Meyer, D.K. Taylor, ACS Nano, 7 (2013) 7992-8002.
[87] M. Acik, G. Lee, C. Mattevi, A. Pirkle, R.M. Wallace, M. Chhowalla, K. Cho, Y. Chabal, The Journal of Physical Chemistry C, 115 (2011) 19761-19781.
[88] W. Chen, L. Yan, Nanoscale, 2 (2010) 559-563.
[89] N. Liu, W. Huang, X. Zhang, L. Tang, L. Wang, Y. Wang, M. Wu, Applied Catalysis B: Environmental, 221 (2018) 119-128.
[90] Y. Hu, J. Wei, Y. Liang, H. Zhang, X. Zhang, W. Shen, H. Wang, Angewandte Chemie International Edition, 55 (2016) 2048-2052.
[91] C. Petit, T.J. Bandosz, Advanced Functional Materials, 21 (2011) 2108-2117.
[92] P.C. Banerjee, D.E. Lobo, R. Middag, W.K. Ng, M.E. Shaibani, M. Majumder, ACS Applied Materials & Interfaces, 7 (2015) 3655-3664.
[93] J. Yang, F. Zhao, B. Zeng, RSC Advances, 5 (2015) 22060-22065.
[94] Z. Guo, M.V. Reddy, B.M. Goh, A.K.P. San, Q. Bao, K.P. Loh, RSC Advances, 3 (2013) 19051-19056.
[95] M. Jahan, Z. Liu, K.P. Loh, Advanced Functional Materials, 23 (2013) 5363-5372.
[96] X. Zhou, W. Huang, J. Shi, Z. Zhao, Q. Xia, Y. Li, H. Wang, Z. Li, Journal of Materials Chemistry A, 2 (2014) 4722-4730.
[97] K. Jayaramulu, K.K.R. Datta, C. Rösler, M. Petr, M. Otyepka, R. Zboril, R.A. Fischer, Angewandte Chemie International Edition, 55 (2016) 1178-1182.

[98] C. Petit, T.J. Bandosz, Advanced Materials, 21 (2009) 4753-4757.
[99] C. Petit, T.J. Bandosz, Journal of Colloid and Interface Science, 447 (2015) 139-151.
[100] D.A. Islam, K. Barman, S. Jasimuddin, H. Acharya, ChemElectroChem, 4 (2017) 3110-3118.
[101] B. Chen, Y. Zhu, Y. Xia, RSC Advances, 5 (2015) 30464-30471.
[102] X. Qiu, X. Wang, Y. Li, Chemical Communications, 51 (2015) 3874-3877.
[103] D. Kim, D.W. Kim, W.G. Hong, A. Coskun, Journal of Materials Chemistry A, 4 (2016) 7710-7717.
[104] G. Yu, J. Xia, F. Zhang, Z. Wang, Journal of Electroanalytical Chemistry, 801 (2017) 496-502.
[105] K. Zhang, A. Xie, M. Sun, W. Jiang, F. Wu, W. Dong, Materials Chemistry and Physics, 199 (2017) 340-347.
[106] J. Xu, S. He, H. Zhang, J. Huang, H. Lin, X. Wang, J. Long, Journal of Materials Chemistry A, 3 (2015) 24261-24271.
[107] S. He, Z. Li, L. Ma, J. Wang, S. Yang, New Journal of Chemistry, 41 (2017) 14209-14216.
[108] M. Jahan, Q. Bao, J.-X. Yang, K.P. Loh, Journal of the American Chemical Society, 132 (2010) 14487-14495.
[109] M. Benzaqui, R.S. Pillai, A. Sabetghadam, V. Benoit, P. Normand, J. Marrot, N. Menguy, D. Montero, W. Shepard, A. Tissot, C. Martineau-Corcos, C. Sicard, M. Mihaylov, F. Carn, I. Beurroies, P.L. Llewellyn, G. De Weireld, K. Hadjiivanov, J. Gascon, F. Kapteijn, G. Maurin, N. Steunou, C. Serre, Chemistry of Materials, 29 (2017) 10326-10338.
[110] X. Cheng, A. Zhang, K. Hou, M. Liu, Y. Wang, C. Song, G. Zhang, X. Guo, Dalton Transactions, 42 (2013) 13698-13705.
[111] B. Seoane, S. Castellanos, A. Dikhtiarenko, F. Kapteijn, J. Gascon, Coordination Chemistry Reviews, 307 (2016) 147-187.
[112] J.H. Lee, J. Jaworski, J.H. Jung, Nanoscale, 5 (2013) 8533-8540.
[113] Y. Yang, W. Wang, H. Li, X. Jin, H. Wang, L. Zhang, Y. Zhang, Materials Letters, 197 (2017) 17-20.
[114] L. Shen, L. Huang, S. Liang, R. Liang, N. Qin, L. Wu, RSC Advances, 4 (2014) 2546-2549.
[115] J. Cai, J.-Y. Lu, Q.-Y. Chen, L.-L. Qu, Y.-Q. Lu, G.-F. Gao, New Journal of Chemistry, 41 (2017) 3882-3886.
[116] J. Li, Q. Wu, X. Wang, Z. Chai, W. Shi, J. Hou, T. Hayat, A. Alsaedi, X. Wang, Journal of Materials Chemistry A, 5 (2017) 20398-20406.
[117] R. Liang, L. Shen, F. Jing, N. Qin, L. Wu, ACS Applied Materials & Interfaces, 7 (2015) 9507-9515.
[118] Z. Bian, J. Xu, S. Zhang, X. Zhu, H. Liu, J. Hu, Langmuir, 31 (2015) 7410-7417.
[119] F. Zhang, L. Liu, X. Tan, X. Sang, J. Zhang, C. Liu, B. Zhang, B. Han, G. Yang, Soft Matter, 13 (2017) 7365-7370.
[120] J. Meng, X. Chen, Y. Tian, Z. Li, Q. Zheng, Chemistry – A European Journal, 23 (2017) 17521-17530.
[121] Y.V. Kaneti, J. Tang, R.R. Salunkhe, X. Jiang, A. Yu, K.C.W. Wu, Y. Yamauchi, Advanced Materials, 29 (2017) 1604898.
[122] S. Dang, Q.-L. Zhu, Q. Xu, Nature Reviews Materials, 3 (2017) 17075.
[123] X. Liang, B. Quan, G. Ji, W. Liu, H. Zhao, S. Dai, J. Lv, Y. Du, ACS Sustainable Chemistry & Engineering, 5 (2017) 10570-10579.
[124] R. Qiang, Y. Du, D. Chen, W. Ma, Y. Wang, P. Xu, J. Ma, H. Zhao, X. Han, Journal of Alloys and Compounds, 681 (2016) 384-393.
[125] B. Ramaraju, C.-H. Li, S. Prakash, C.-C. Chen, Chemical Communications, 52 (2016) 946-949.
[126] X. Cao, B. Zheng, X. Rui, W. Shi, Q. Yan, H. Zhang, Angewandte Chemie International Edition, 53 (2014) 1404-1409.
[127] Q. Qu, T. Gao, H. Zheng, X. Li, H. Liu, M. Shen, J. Shao, H. Zheng, Carbon, 92 (2015) 119-125.
[128] J. Xu, W. Zhang, Y. Chen, H. Fan, D. Su, G. Wang, Journal of Materials Chemistry A, 6 (2018) 2797-2807.

[129] X. Cao, B. Zheng, W. Shi, J. Yang, Z. Fan, Z. Luo, X. Rui, B. Chen, Q. Yan, H. Zhang, Advanced Materials, 27 (2015) 4695-4701.
[130] L. Yan, H. Jiang, Y. Xing, Y. Wang, D. Liu, X. Gu, P. Dai, L. Li, X. Zhao, Journal of Materials Chemistry A, 6 (2018) 1682-1691.
[131] K. Jayaramulu, J. Masa, O. Tomanec, D. Peeters, V. Ranc, A. Schneemann, R. Zboril, W. Schuhmann, R.A. Fischer, Advanced Functional Materials, 27 (2017) 1700451-n/a.
[132] X. Fang, L. Jiao, R. Zhang, H.-L. Jiang, ACS Applied Materials & Interfaces, 9 (2017) 23852-23858.
[133] L. Jiao, Y.-X. Zhou, H.-L. Jiang, Chemical Science, 7 (2016) 1690-1695.
[134] J. Wei, Y. Hu, Y. Liang, B. Kong, J. Zhang, J. Song, Q. Bao, G.P. Simon, S.P. Jiang, H. Wang, Advanced Functional Materials, 25 (2015) 5768-5777.
[135] Q. Niu, J. Guo, Y. Tang, X. Guo, J. Nie, G. Ma, Electrochimica Acta, 255 (2017) 72-82.
[136] H.x. Zhong, J. Wang, Y.w. Zhang, W.l. Xu, W. Xing, D. Xu, Y.f. Zhang, X.b. Zhang, Angewandte Chemie International Edition, 53 (2014) 14235-14239.
[137] J. Wei, Y. Hu, Y. Liang, B. Kong, Z. Zheng, J. Zhang, S.P. Jiang, Y. Zhao, H. Wang, Journal of Materials Chemistry A, 5 (2017) 10182-10189.
[138] Y. Hou, Z. Wen, S. Cui, S. Ci, S. Mao, J. Chen, Advanced Functional Materials, 25 (2015) 872-882.
[139] C. Xing, Y. Liu, Y. Su, Y. Chen, S. Hao, X. Wu, X. Wang, H. Cao, B. Li, ACS Applied Materials & Interfaces, 8 (2016) 15430-15438.
[140] J. Lee, J. Kim, T. Hyeon, Advanced Materials, 18 (2006) 2073-2094.
[141] F.J. Martín-Jimeno, F. Suárez-García, J.I. Paredes, M. Enterría, M.F.R. Pereira, J.I. Martins, J.L. Figueiredo, A. Martínez-Alonso, J.M.D. Tascón, ACS Applied Materials & Interfaces, 9 (2017) 44740-44755.
[142] B.C. Brodie, Philosophical Transactions of the Royal Society of London, 149 (1859).
[143] S. Stankovich, D.A. Dikin, R.D. Piner, K.A. Kohlhaas, A. Kleinhammes, Y. Jia, Y. Wu, S.T. Nguyen, R.S. Ruoff, Carbon, 45 (2007) 1558-1565.
[144] A. Ganguly, S. Sharma, P. Papakonstantinou, J. Hamilton, The Journal of Physical Chemistry C, 115 (2011) 17009-17019.
[145] C. Gómez-Navarro, J.C. Meyer, R.S. Sundaram, A. Chuvilin, S. Kurasch, M. Burghard, K. Kern, U. Kaiser, Nano Letters, 10 (2010) 1144-1148.
[146] X. Li, Z. Le, X. Chen, Z. Li, W. Wang, X. Liu, A. Wu, P. Xu, D. Zhang, Applied Catalysis B: Environmental, 236 (2018) 501-508.
[147] M.S. Dresselhaus, A. Jorio, M. Hofmann, G. Dresselhaus, R. Saito, Nano Letters, 10 (2010) 751-758.
[148] G. Bottari, M.Á. Herranz, L. Wibmer, M. Volland, L. Rodríguez-Pérez, D.M. Guldi, A. Hirsch, N. Martín, F. D'Souza, T. Torres, Chemical Society Reviews, 46 (2017) 4464-4500.
[149] S. Claramunt, A. Varea, D. López-Díaz, M.M. Velázquez, A. Cornet, A. Cirera, The Journal of Physical Chemistry C, 119 (2015) 10123-10129.
[150] D. López-Díaz, M. López Holgado, J.L. García-Fierro, M.M. Velázquez, The Journal of Physical Chemistry C, 121 (2017) 20489-20497.
[151] Y. Wei, Z. Hao, F. Zhang, H. Li, Journal of Materials Chemistry A, 3 (2015) 14779-14785.
[152] W. Cai, R.D. Piner, F.J. Stadermann, S. Park, M.A. Shaibat, Y. Ishii, D. Yang, A. Velamakanni, S.J. An, M. Stoller, J. An, D. Chen, R.S. Ruoff, Science, 321 (2008) 1815-1817.
[153] L.B. Casabianca, M.A. Shaibat, W.W. Cai, S. Park, R. Piner, R.S. Ruoff, Y. Ishii, Journal of the American Chemical Society, 132 (2010) 5672-5676.
[154] E. Pump, J. Viger-Gravel, E. Abou-Hamad, M.K. Samantaray, B. Hamzaoui, A. Gurinov, D.H. Anjum, D. Gajan, A. Lesage, A. Bendjeriou-Sedjerari, L. Emsley, J.-M. Basset, Chemical Science, 8 (2017) 284-290.
[155] W.-C. Liao, B. Ghaffari, C.P. Gordon, J. Xu, C. Copéret, Current Opinion in Colloid & Interface Science, 33 (2018) 63-71.

[156] P. He, J. Xu, V.V. Terskikh, A. Sutrisno, H.-Y. Nie, Y. Huang, The Journal of Physical Chemistry C, 117 (2013) 16953-16960.
[157] G.P.M. Bignami, Z.H. Davis, D.M. Dawson, S.A. Morris, S.E. Russell, D. McKay, R.E. Parke, D. Iuga, R.E. Morris, S.E. Ashbrook, Chemical Science, 9 (2018) 850-859.
[158] D. Li, M.B. Müller, S. Gilje, R.B. Kaner, G.G. Wallace, Nature Nanotechnology, 3 (2008) 101.
[159] O.C. Compton, S.T. Nguyen, Small, 6 (2010) 711-723.
[160] B. Tang, Z. Xiong, X. Yun, X. Wang, Nanoscale, 10 (2018) 4113-4122.
[161] J.-J. Shao, W. Lv, Q.-H. Yang, Advanced Materials, 26 (2014) 5586-5612.
[162] S. Bonakala, A. Lalitha, J.E. Shin, F. Moghadam, R. Semino, H.B. Park, G. Maurin, ACS Applied Materials & Interfaces, 10 (2018) 33619-33629.